

Short Communication

Electrochemical Deposition of $\text{Cu}_2\text{ZnSnSe}_4$ Thin Film on Mo-glass Electrode from Tartaric Acid

K.A. Urazov*, V.I. Yaskevich, B.E. Myrzabekov

D.V. Sokolskiy Institute of Fuels, Catalysis and Electrochemistry, Almaty, 050010, Kazakhstan

*E-mail: u_kazhm@mail.ru

Received: 1 April 2022 / *Accepted:* 13 May 2022 / *Published:* 4 July 2022

The findings of cyclic voltammetry investigation of copper(II), zinc(II), tin(IV), selenium(IV) ions simultaneous electrochemical reduction on the molybdenum disk electrode from a tartaric acid-based electrolyte are provided. $\text{Cu}_2\text{ZnSnSe}_4$ (CZTSe) thin films were produced in the potentiostatic mode on Mo/glass substrates and their characteristics were studied. The prepared films have a rough surface and are formed from large particles 1–2 μm in size, which consist of small spherical particles with an average size of 200–500 nm. The phase composition and the band gap energy of the obtained thin films were investigated. It was shown that electrodeposited CZTSe thin film has photoactivity.

Keywords: cyclic voltammetry, electrodeposition, $\text{Cu}_2\text{ZnSnSe}_4$, thin film, kestrite, solar cell.

1. INTRODUCTION

The development of cheap and technological techniques for producing non-toxic semiconductor materials, which are used as efficient light absorbers in solar cells, is important to the future progress of thin-film photovoltaics. These materials include the four-component CZTSe thin film with the kesterite structure [1, 2]. Along with its good optical properties, this material's advantages include its abundance and low cost of components in the crust of the earth [3–8].

To date, numerous methods for producing CZTSe thin films have been developed, including sputtering [9], chemical deposition [10], electrochemical deposition [11–15], and others. Electrochemical deposition is one of the most promising methods for obtaining thin films owing to the relatively simplicity of the technology and equipment, as well as the ability to control the chemical composition and thickness of the coating by changing the potential or current. The electrochemical production of CZTSe thin film can be performed in two ways: 1) simultaneous electrodeposition of all components in one stage, and 2) sequential electrodeposition of metal layers, followed by selenization. These methods have both disadvantages and advantages. In contrast to sequential deposition, the

advantage of simultaneous electrodeposition is the ability to obtain a thin film with a single-phase structure free of binary or ternary compound impurities. Electrochemical methods have also been applied to successfully produce thin films as CuInSe₂ [16] and Cu(In,Ga)(Se,S)₂ [17].

The aim of the research is to investigate the properties of the CZTSe thin films formed on a Mo-coated glass by one-step electrochemical deposition from a tartaric acid-based electrolyte.

2. EXPERIMENTAL

The electrochemical behavior of copper(II), zinc(II), tin(IV), and selenium(IV) ions in an electrolyte solution containing 0.1 M tartaric acid was studied using the method of cyclic voltammetry with a potential sweep rate 20 mV/sec. Electrodeposition of CZTSe thin films was performed at a potential -600 mV with stirring in electrolyte solution containing 0.002M CuSO₄·5H₂O, 0.01M ZnSO₄·7H₂O, 0.01M SnCl₄·5H₂O and 0.005M NaHSeO₃ and 0.1 M tartaric acid (C₄H₆O₆). Electrochemical experiments were carried out using a potentiostat Gill AC at room temperature in a three-electrode cell, which consists of a molybdenum disk electrode (S=0.07 cm²) or Mo/glass substrate as a working electrode, a Pt counter electrode, and Ag/AgCl reference electrode. The film electrodeposited was washed with distilled water, dried in air, and annealed at 450°C in Ar atmosphere for 30 min.

The chemical composition and surface topography of prepared thin films were studied using JSM-6600 SEM with EDAX determination (JEOL) and JSPM-5200 atomic force microscopy (JEOL). Crystal structure was investigated by XRD analysis using a DRON-4-07 (Bourestnik) diffractometer with a copper X-Ray tube.

Photoelectrochemical (PEC) analysis of prepared CZTSe thin films was performed in a three-electrode cell using an 0.1 M Na₂SO₄ electrolyte. CZTSe/Mo/glass sample was working electrode, a Pt-coil and Ag/AgCl electrode used as the counter electrode and reference electrode, respectively. A Gill AC potentiostat was used to registration voltammograms. Polychromatic light source with an intensity 80 mW cm⁻² was used for chopped illumination.

3. RESULTS AND DISCUSSION

The electrodeposition of a four-component compound containing copper, zinc, and tin selenides in a single step is quite difficult. Therefore, the simultaneous electrochemical reduction of copper, zinc, and tin selenides on a molybdenum disk electrode was studied using cyclic voltammetry in a tartaric acid-based electrolyte. Previously, in [18], we discovered that polarization of a molybdenum disk electrode in acidic solutions is possible within a potential range of -600 ÷ +300 mV. At more negative than -600 mV potentials, hydrogen evolution begins on the molybdenum disk electrode, and the electrode is passivated if the potential is higher than +300 mV. From a background electrolyte based on 0.1M tartaric acid, polarization of the molybdenum electrode into the cathode region is possible up to -600 mV, as shown in Figure 1.

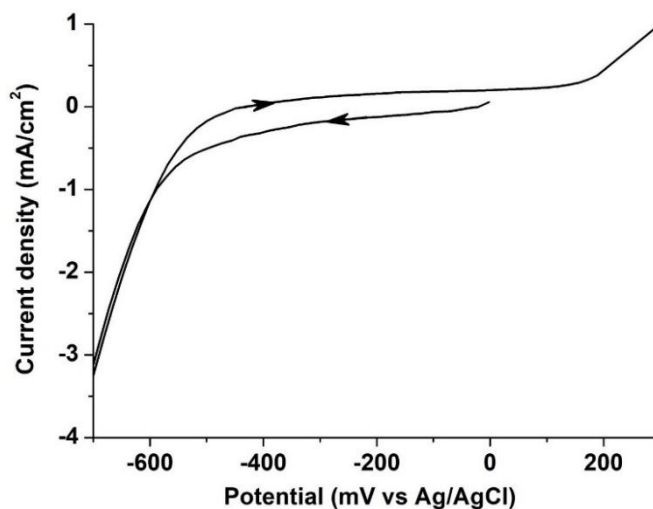


Figure 1. Voltammetry curve for Mo-disk electrode in 0.1 M $C_4H_6O_6$.

The electrochemical reduction of Cu(II) from an electrolyte solution containing 0.1 M tartaric acid proceeds in a negative potential area, as was shown in [19]. Tin and zinc ions didn't show any cathodic or anodic peaks in the interval between 0 ÷ -600 mV. Figure 2 shows that with the joint reduction of all four components, a cathodic peak appears in the potential interval 0 ÷ -400 mV and corresponds to joint reduction of copper and selenium [19]. The cathodic peak with a maximum at -420 most likely corresponds to the reduction of tin with selenium. The curve shows a cathodic peak at -500 mV, close to the hydrogen evolution potential, where the reduction process of zinc can take place. The synthesis of a four-component metal compound with selenium probably passes through the stages of binary compound formation. Additionally, near the electrode, negatively charged selenide ions (Se^{2-}) can join a reaction with positively charged metal ions, forming metal selenides. Based on the analysis of the cyclic voltammetry investigation, the optimal mode for the deposition of CZTSe films was chosen.

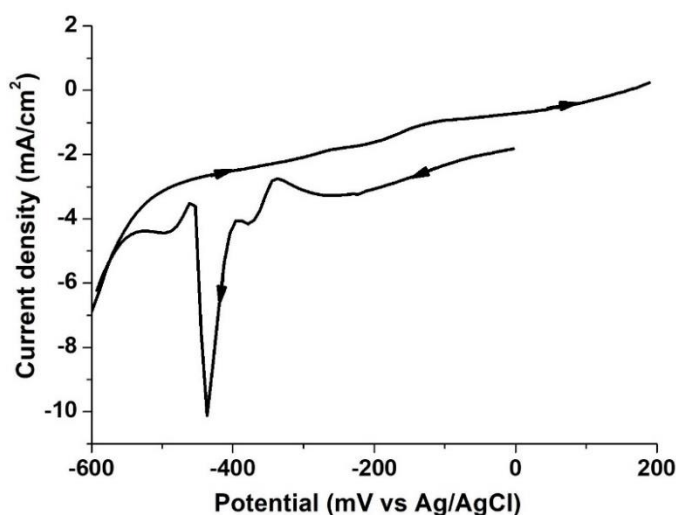


Figure 2. Voltammetry curve for Mo-disk electrode in 0.1 M $C_4H_6O_6$ and 0.002M $CuSO_4 \cdot 5H_2O$ + 0.01M $ZnSO_4 \cdot 7H_2O$ + 0.01M $SnCl_4 \cdot 5H_2O$ + 0.005M $NaHSeO_3$.

Figure 3 shows a SEM micrograph of the surface and elemental mapping of an electrodeposited CZTSe thin film after annealing. The heat treatment process is very important for the formation of kesterite thin films [20]. It's also important to note that the annealing process has an impact on the surface topography of the obtained films. A SEM micrograph demonstrates that the surface topography is formed of spherical grains of varied sizes, ranging from 0.5 μm to 2 μm . EDX elemental mapping confirms the constituent elements and homogenous distribution of them as presented in Figure 3.

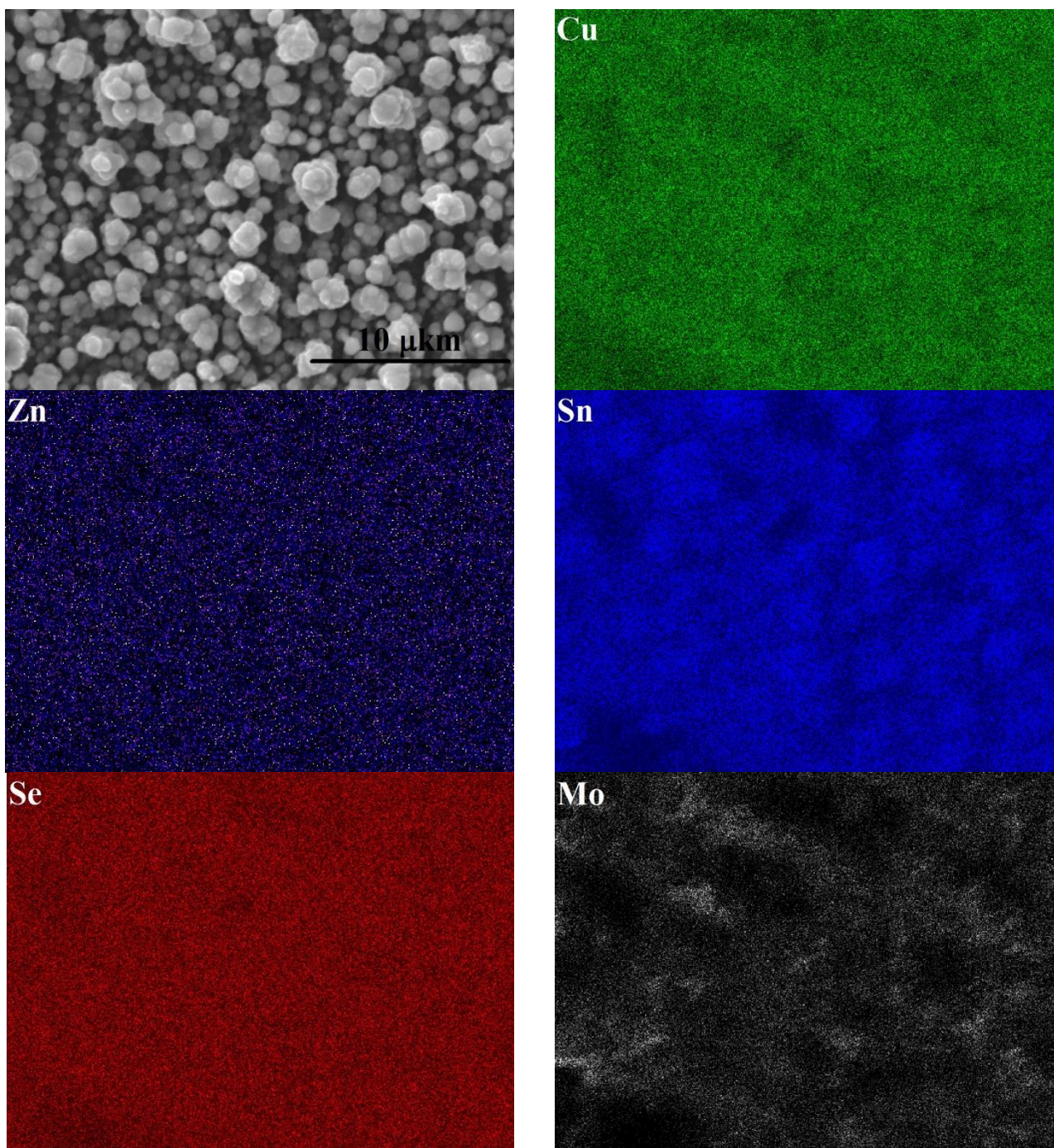


Figure 3. SEM micrograph and EDX elemental mapping analysis of CZTSe/Mo/glass.

Using atomic force microscopy, the surface topography of electrodeposited CZTSe films was studied and presented in Figure 4. An investigation of the topography of the obtained film indicated that the surface has a different microrelief.

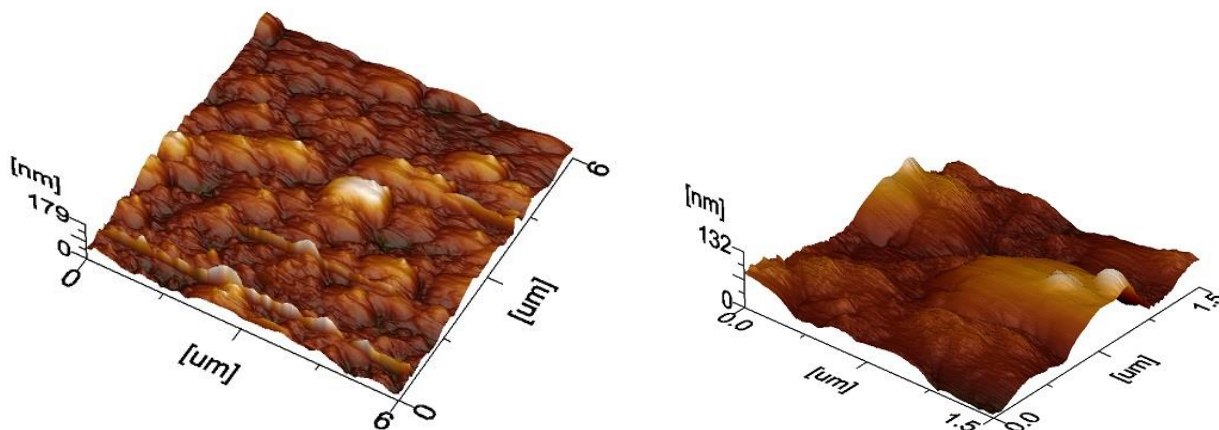


Figure 4. ACM images of the CZTSe thin film’s surface topography.

On the surface of electrodeposited CZTSe, a localized grainy structure as well as erosion zones can be observed, which form clusters $0.5 \times 1 \mu\text{m}$ in size and 130-180 nm high during deposition. The observed grains are rounded. Nanometer pores are also seen on the surface topography of the obtained film, which could be caused by hydrogen released during the reduction of the metal from the electrolyte.

Table 1 shows the results of the chemical composition analysis of the CZTSe film.

Table 1. Elemental analysis of the electrodeposited CZTSe film.

| Substrate | Element composition, atomic% | | | | Ratio of elements | |
|-----------|------------------------------|------|------|------|-------------------|-------|
| | Cu | Zn | Sn | Se | Cu/(Zn+Sn) | Zn/Sn |
| Mo/glass | 19.6 | 10.6 | 14.6 | 55.2 | 0.77 | 0.73 |

The X-Ray diffraction results in Figure 5 show three main peaks, which correspond with the CZTSe phase (JCPDS 52-0868). Peaks at 40.5° and 58.6° are assigned to the Mo substrate.

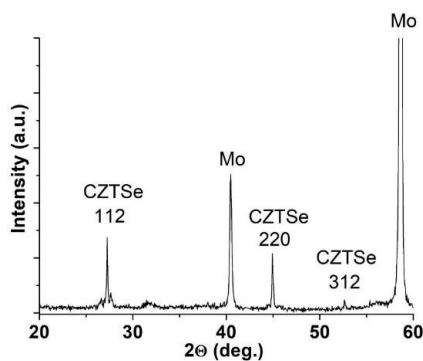


Figure 5. XRD pattern of CZTSe/Mo/glass.

The lattice parameters of CZTSe were calculated from the XRD results and are presented in Table 2.

Table 2. Lattice parameters of electrodeposited CZTSe.

| Substrate | a , Å | c , Å |
|-----------|-------------------|--------------------|
| Mo/glass | 5.696 ± 0.003 | 11.339 ± 0.010 |

The band gap, $E_g = 1.32$ eV, was determined by studying the optical characteristics of electrodeposited CZTSe using the IR spectroscopy method.

Photoelectrochemical analysis was used to investigate the photocurrent-voltage measurements of electrodeposited CZTSe under chopped illumination in a 0.1 M Na_2SO_4 electrolyte. The results are presented in Figure 6. Photoactivity was discovered in electrodeposited CZTSe. A cathodic current was generated by CZTSe/Mo/glass, indicating that it was a p-type semiconductor electrode.

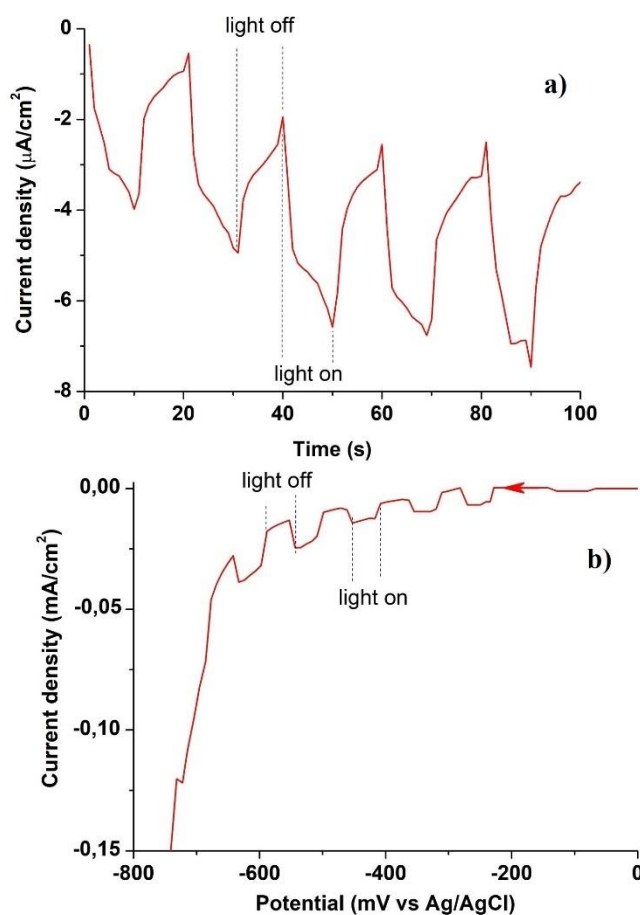


Figure 6. Chronoamperometric dependence (a) and voltammogram (b) for CZTSe/Mo/glass under chopped illumination.

Photocurrent for CZTSe/Mo/glass is the same as the photocurrent generated by CZTSe/FTO/glass, which we previously reported in [21]. The values of photocurrents for CZTSe/Mo/glass was 3.0-3.5 $\mu\text{A}/\text{cm}^2$. We propose that the transient spike can be related to sluggish charge transfer due to surface roughness.

4. CONCLUSION

A one-step electrochemical deposition of CZTSe in potentiostatic mode was performed based on the voltammetry investigation of copper(II), zinc(II), tin(IV), and selenium(IV) ions on the molybdenum disk electrode in a tartaric acid-based electrolyte. Heat treatment in an Ar atmosphere was used to optimize the crystal structure of the CZTSe thin film. Elemental, structural, and photoelectrochemical analyses were performed to characterize the properties of the prepared thin films. The chemical composition was observed that is close to stoichiometric. The phase structure was confirmed by XRD. The surface topography of the obtained film has microrelief with a grainy structure. The electrodeposited CZTSe thin film demonstrated photoactivity.

ACKNOWLEDGEMENT

This work was supported by the Science Committee of the Ministry of Education and Science, Kazakhstan (Grant No. AP08051961).

References

1. S. Siebentritt, S. Schorr, *Prog. Photovolt: Res. Appl.*, 20 (2012) 512-519.
2. M. He, C. Yan, J. Li, M. P. Suryawanshi, J. Kim, M. A. Green, X. Hao, *Adv. Sci.*, 8 (2021) 2004313.
3. J. Li, Y. Huang, J. Huang, G. Liang, Y. Zhang, G. Rey, F. Guo, Z. Su, H. Zhu, L. Cai, K. Sun, Y. Sun, F. Liu, S. Chen, X. Hao, Y. Mai, M. A. Green, *Adv. Mater.*, 32 (2020) 2005268.
4. J. Henry, K. Mohanraj, G. Sivakumar, *Vacuum*, 156 (2018) 172-180.
5. S. Giraldo, M. Placidi, E. Saucedo, *Advanced Micro- and Nanomaterials for Photovoltaics*, Elsevier, (2019) Netherlands.
6. P.M. Salome, P.A. Fernandes, J.P. Leitao, *J. Mater. Sci.*, 49 (2014) 7425-7436.
7. M. Benaicha, M. Hamla, S. Derbal, *Int. J. Electrochem. Sci.*, 11 (2016) 4909-4921.
8. O. Volobujeva, S. Bereznev, J. Raudoja, K. Otto, M. Pilvet, E. Mellikov, *Thin Solid Films*, 535 (2013) 48-51.
9. Y. Wei, D. Zhuang, M. Zhao, Q. Gong, R. Sun, L. Zhang, X. Lyu, X. Peng, G. Ren, Y. Wu, J. Wei, *J. Alloy. Compd.*, 755 (2018) 224-230.
10. J. Li, G. Chen, C. Xue, X. Jin, W. Liu, C. Zhu, *Sol. Energ. Mat. Sol. C.*, 137 (2015) 131-137.
11. Z. Zhang, Q. Gao, J. Guo, Y. Zhang, Y. Han, J. Ao, M. Jeng, F. Liu, W. Liu, Y. Zhang, *Solar RRL*, 4 (2020) 2000059.
12. J.-O. Jeon, K.D. Lee, L. Seul Oh, S.-W. Seo, D.-K. Lee, H. Kim, J.-h. Jeong, M.J. Ko, B. Kim, H.J. Son, J.Y. Kim, *ChemSusChem*, 7 (2014) 1073-1077.
13. M. Meng, L. Wan, P. Zou, S. Miao, J. Xu, *Appl. Surf. Sci.*, 273 (2013) 613-616.
14. L. Vauche, J. Dubois, A. Laparre, F. Mollica, R. Bodeux, S. Delbos, C.M. Ruiz, M. Pasquinelli, F. Bahi, T.G. de Monsabert, S. Jaime, S. Bodnar, P.-P. Grand, *Phys. Status Solidi A*, 211 (2014) 2082-2085.
15. J. Li, T. Ma, M. Wei, W. Liu, G. Jiang, C. Zhu, *Appl. Surf. Sci.*, 258 (2012) 6261-6265.

16. R. Chandran, R. Pandey, A. Mallik, *Mater. Lett.*, 160 (2015) 275-277.
17. V. Bermudez, *Sol. Energy*, 175 (2018) 2-8.
18. M.B. Dergacheva, K.A. Urazov, N.V. Pen'kova, *Russ. J. Appl. Chem.*, 83 (2010) 653-658.
19. M.B. Dergacheva, A.E. Nurtazina, K.A. Urazov, N.N. Gudeleva, V.I. Yaskevich, V.P. Grigor'eva, *Russ. J. Appl. Chem.*, 91 (2018) 778-784.
20. M.A. Olgar, B.M. Başol, Y. Atasoy, M. Tomakin, G. Aygun, L. Ozyuzer, E. Bacaksız, *Thin Solid Films*, 624 (2017) 167-174.
21. K. Urazov, M. Dergacheva, A. Tameev, O. Gribkova, *J Solid State Electr*, 25 (2021) 237-245.

© 2022 The Authors. Published by ESG (www.electrochemsci.org). This article is an open access article distributed under the terms and conditions of the Creative Commons Attribution license (<http://creativecommons.org/licenses/by/4.0/>).